Published in final edited form as:
NMR Biomed. 2012 April ; 25(4): 498–505. doi:10.1002/nbm.1760.

Quantitative pharmacologic MRI in mice

Teodora-Adriana Perles-Barbacaru[1], **Daniel Procissi**[1], **Andrey V. Demyanenko**[1], and **Russell E. Jacobs**[1]

[1]Biological Imaging Center, Beckman Institute, California Institute of Technology, Pasadena, CA 91125

Abstract

Pharmacologic MRI (phMRI) uses functional MRI techniques to provide a non-invasive *in vivo* measurement of the hemodynamic effects of drugs. The cerebral blood volume change (ΔCBV) serves as a surrogate for neuronal activity via neurovascular coupling mechanisms. By assessing the location and time course of brain activity in mouse mutant studies, phMRI can provide valuable insights into how different behavioral phenotypes are expressed in differing brain activity response to drug challenge. In this report, we evaluate the utility of three different intravascular ultrasmall superparamagnetic iron oxide (USPIO) contrast agents for phMRI using a gradient-echo technique with temporal resolution of one minute at high magnetic field. The tissue half life of the USPIOs was studied using a nonlinear detrending model. All three studied USPIOs are candidates for CBV weighted phMRI-experiments, with r_2/r_1 ratios ≥ 20 and apparent half-lives ≥ 1.5 h at the described doses. An echo time of about 10 ms or longer results in a fCNR > 75 after USPIO injection, with negligible decrease during 1.5 to 2 hours. phMRI experiments were conducted at 7T using cocaine as a psychotropic substance and acetazolamide, a global vasodilator, as a positive control. Cocaine acts as a dopamine-serotonin-norepinephrine reuptake inhibitor, increasing extracellular concentrations of these neurotransmitters and thus increasing dopaminergic, serotonergic and noradrenergic neurotransmission. phMRI indicated that CBV was reduced in the normal mouse brain after cocaine challenge, with largest effects in nucleus accumbens, while after acetazolamide the blood volume was increased in both cerebral and extra-cerebral tissue.

Introduction

Pharmacological magnetic resonance imaging (phMRI) is well suited to monitor drug action in the brain dynamically and noninvasively; mapping brain systems and networks targeted by psychoactive drugs (1, 2). phMRI measures the hemodynamic responses to a pharmacological challenge, and thus probes the activity of neuronal pathways targeted by the drug based on the neurovascular consequences of changed neuronal (and vascular) activities (3–5). This technique has the potential to elucidate the underlying changes in regional brain activities in mouse models of disorders related to altered brain function. However, small brain size, rapid metabolic rates, susceptibility artifacts, and the need for anesthesia render functional MRI in mice challenging. In phMRI the sensitivity to functional changes is enhanced with T_2* contrast agents such as ultrasmall superparamagnetic iron oxide particles (USPIO) that exhibit long circulation times (6). The effect of the particles is so large that most of the MRI signal arises from the cerebral blood volume (CBV) with insignificant blood oxygen level dependent (BOLD) or blood flow contributions. Studies

Corresponding author: Russell E. Jacobs, PhD, Caltech M/C 139-74, 1200 E. California Blvd, Pasadena, CA 91125, Phone (626) 395-2849, FAX (626) 449-5163, rjacobs@caltech.edu.

using this technique are typically performed with rats (4, 5, 7) or nonhuman primates (3), although there have been a few studies in mice (8–10).

We have adapted the technique to meet the requirements of mouse imaging, balancing sequence parameters and contrast agent dose to maintain a reasonable signal to noise ratio (SNR), avoid excessive susceptibility artifacts in the brain regions of interest (ROIs) and achieve good sensitivity to the CBV change at a time resolution of < 1 minute and spatial resolution of < 0.2 mm. We optimized USPIO choice and dose to yield a procedure with short echo times. Three contrast agents were evaluated: P904, a new USPIO from Guerbet Research (Aulnay-Sous-Bois, France), monocrystalline iron oxide nanoparticle (MION) (Massachusetts General Hospital, Boston, MA) and MoldayION (BioPAL, MA). Although this study was focused on mouse imaging, the usefulness of P904 for the CBV weighted technique was investigated with the idea in mind that this new USPIO may provide useful properties for clinical use in humans.

A number of important classes of medications used in the treatment of psychiatric disorders and many drugs of abuse target plasma membrane reuptake transporters for the monoamine neurotransmitters dopamine, norepinephrine, and serotonin inhibiting the reuptake of the released neurotransmitters (11). Dopamine systems including cortico-mesolimbic systems are crucial for normal reward-seeking behavior and are likely to make major contributions to the development of addiction (12). In the present report, we have used the CBV weighted phMRI approach to map the hemodynamic response to an acute cocaine challenge in normal mice.

Material and Methods

Animals

Female C57BL/6J mice were used the *in vivo* phMRI experiments. Scans with MION employed 5 animals, those with MoldayION used 4 animals, and those with P904 used 6 animals. All experiments were performed in accordance with protocols approved by the Institutional Animal Care and Use Committee of the California Institute of Technology.

Contrast agents

MION—Dextran coated monocrystalline iron oxide nanoparticle with a hydrodynamic diameter ~ 40 nm (13) was purchased from Harvard Medical School (Massachusetts General Hospital, Boston, MA) at a concentration of 17 mg/ml. A volume of 2 μl MION/g body weight (35 mg/kg) was introduced via tail vein injection (IV) (N = 5 mice).

MoldayION—The colloidal magnetite MoldayION (diameter ≈ 30 nm) was purchased from BioPAL (Worcester, MA) at a concentration of 10 mg/ml (14). 2.5 μl/g body weight (25 mg/kg) was injected IV (N = 4 mice).

P904—P904 (Guerbet Research, Aulnay-Sous-Bois, France) is a research prototype USPIO with a hydrodynamic diameter of 25 to 30 nm and a glucose derivative coating designed for macrophage and vascular imaging applications (15). It was provided as a 500 mM (≈ 28 mg/ml) solution and was diluted to 3 mg/ml and 6 mg/ml in sterile normal saline solution for IV injection. A volume of ≈ 4.2 μl/g body weight was injected IV resulting in a dose of 15 mg/kg (N = 4 mice) and 25 mg/kg (N = 2 mice).

Drugs

Cocaine hydrochloride (Sigma-Aldrich, MO) was dissolved in normal saline solution (5 mg/ml) for IP injection at a dose of 30 mg/kg. The carbonic anhydrase inhibitor and vasodilator

acetazolamide (Diamox, Bedford Laboratories, OH) was dissolved in normal saline solution (16 mg/ml) and injected IP at a dose of 160 mg/kg. Cocaine dosage was established in pilot experiments that did not involve MRI. In these experiments, the electrocardiogram, respiration and expired CO_2 (MicroCapStar CO_2 Monitor, IITC Life Science Inc., CA) of mice were continuously recorded during cocaine intraperitoneal injection (IP). Criteria for the choice of the cocaine dose were no arousal from anesthesia and stable physiologic parameters after injection. Behavioral changes have been reported starting at a cocaine dose of 5 mg/kg IP in conscious mice (16) while cocaine induced seizures start to appear at 70 mg/kg IP. Doses of 20 to 40 mg/kg IP increase striatal and nucleus accumbens dopamine levels 3-fold in wild type mice (17, 18). Thus, the dose of 30 mg/kg used here is well within known limits.

In vitro relaxation time measures

The longitudinal T_1 and transverse T_2 relaxation times of several contrast agent concentrations (8 different concentrations for MION and P904; 6 for MoldayION) up to 0.3 mg Fe^{3+}/ml (= 5.37 mM Fe^{3+}) in rat plasma at 37°C were measured in a horizontal bore Bruker Biospec/Avance 7T/30 cm small animal MR system and a vertical bore Bruker BioSpin Avance DRX500 11.7T/8.9 cm MR system. A spectroscopic inversion recovery pulse sequence with 12 inversion times and echo time TE = 50 μs, and a Hahn spin-echo pulse sequence with 12 TE and a repetition time TR > $5T_1$ were used. Each measurement was repeated three times. The longitudinal r_1- and transverse r_2-relaxivities were determined as the slope of a linear regression.

In vivo phMRI

In vivo MRI experiments were performed at 7T using a custom made 12-rung linear birdcage RF coil (length 45 mm, inner diameter 26 mm) for transmission and reception. The mice were positioned prone in a plastic cradle with an integral head mask providing 1.5 to 1.7% isoflurane in N_2/O_2 70%/30% and incorporated ECG electrodes for the front paws and tail. Rectal temperature (Opsens OTG-M, Canada) and respiration (BIOPAC Systems, CA) were monitored continuously. Simultaneous recording of the electrocardiogram during gradient echo imaging was not always reliable, but the heart rate at the start and end of the acquisition were compared. The body temperature was maintained between 36 and 38°C using heated air passed through the RF coil and a cylindrical plastic extension that covered the mouse body to prevent loss of the warm air. The isoflurane level was adjusted to achieve respiratory rates of 80 to 120 breaths per minute and was not changed during image acquisition. The mice were fitted with tail vein catheters for IV USPIO injection and IP catheters for drug injection. Both catheters had extension lines with total volumes of 200 μl and were preloaded with USPIO and drug in normal saline solution before positioning the mouse in the magnet. All USPIO and drugs were injected by flushing the IV/IP catheter with 250 μl saline solution over a duration of 1 minute while the mouse was positioned inside the scanner. phMRI experiments were begun only after animal temperature (36–38°C), respiration, and heart rate (500–750 beats per minute) had stabilized. Further, scans were terminated if physiological parameters strayed outside normal range or anesthesia became ineffective at low doses.

An autoshiming routine resulted in a ^1H linewidth of < 0.13 ppm (FWHM) in a cube of 4 × 4 × 4 mm^3 brain tissue. After obtaining stable physiologic conditions, relative CBV maps were obtained based on the intravascular susceptibility effect of the USPIO (4, 19).

For each brain, 14 contiguous axial 0.75 mm thick slices with a field of view of 18 × 18 mm^2 were acquired from the olfactory bulb to the cerebellum using a 2D multiple gradient echo sequence with TR = 600 ms, flip angle = 35°, 100 × 100 matrix, spectral line width 60

kHz, four echoes at TE = 2.5, 6.0, 9.5 and 13 ms, and an acquisition time of 1 minute per repetition.

Figure 1 illustrates the phMRI protocol: R_2* weighted images were acquired for 20 minutes; 20 post-contrast baseline acquisitions were acquired; cocaine was administered IP; 80 minutes of scans were acquired; acetazolamide was administered IP and imaging continued for another 80 acquisitions. Due to the length of the imaging protocol we used rather short baseline intervals (20 minutes). In experiments performed to examine the *in vivo* properties of the USPIOs only one pharmacological challenge was performed consisting of IP injection of cocaine or normal saline solution, up to 30 minutes baseline intervals were used and the CBV was monitored for at least 90 minutes after pharmacological challenge.

MRI data analysis

Pre-contrast and post-contrast images were automatically coregistered with a 2D rigid body (3 parameters) model using Automated Image Registration (AIR) software (20). Image analysis was performed with ImageJ (21). No spatial or temporal smoothing was applied to the data.

ROIs were outlined manually according to a mouse brain atlas (22) on the first echo (TE = 2.5 ms) images of the multiple gradient echo sequence with the help of the images at TE ≥ 6 ms for better visualization of the ventricles and white matter. They were then copied to the other echoes for signal analysis. Perles-Barbacaru et al (23) shows outlines of the ROIs analyzed.

For each USPIO, we quantified the signal decrease upon injection and estimated the tissue washout rate of the contrast agent, both of which determine the sensitivity of the technique to functional CBV changes. The relative signal decrease upon contrast agent (CA) administration:

$$1 - S_{postCA}/S_{preCA} \tag{1}$$

depends on the relaxivity of the contrast agent and its tissue concentration. These factors determine the transverse relaxation rate change

$$\Delta R_2^* = -\frac{1}{TE}\ln\left(S_{postCA}/S_{preCA}\right), \tag{2}$$

where TE is the echo time, S_{preCA} is the mean signal intensity prior to contrast agent injection and S_{postCA} is the signal intensity averaged over the first five acquisitions after contrast agent injection (Figure 1).

The apparent tissue washout rate of the contrast agent was estimated by fitting the signal intensity after contrast agent injection during two time intervals prior to and 60 to 80 minutes after pharmacological challenge (Figure 1) to a two parameter model:

$$S_0(t) = S_{preCA}\exp\left(-TE\cdot\kappa\cdot\exp\left(-\frac{t}{\tau}\right)\right) \tag{3}$$

where S_{preCA} is defined as above. The fitting parameter κ provides an estimate of the initial ΔR_2* following USPIO injection, while τ is the apparent washout rate of the contrast agent from the tissue. In this model we assume negligible T_1-effects, an instantaneous USPIO bolus and monoexponential decay in the plasma, since USPIO is confined to the intravascular compartment. The outer exponential results from the R_2* weighting (24). The

return of the CBV to the pre-challenge value within 60 minutes is an assumption supported by microdialysis studies in rats ((25), and behavioral studies in mice following IP cocaine injection (26).

The relative CBV change (ΔCBV) is calculated by assuming a linear relationship between CBV and ΔR_2^* (4):

$$\Delta CBV(t) = \frac{\ln(S_0(t)/S(t))}{\ln\left(S_{preCA}/S_0(t)\right)}, \quad (4)$$

where $S_0(t)$ represents the fit to the signal time-course after contrast agent injection under resting conditions with no drug challenge (Eq. 3). S(t) refers to the measured signal. We computed parametric maps of the transverse relaxation rate change κ upon contrast agent injection, of the apparent tissue washout rate τ and of the ΔCBV after pharmacologic challenge.

Quantitative analysis of the ΔCBV upon drug injection was also performed on a number of cerebral ROIs that are thought to form the drug reward circuitry. We analyzed ROIs in the motor and somatosensory cortex (CTX), nucleus accumbens (ACB), caudate putamen (CP), hippocampal formation (HPF), thalamic nuclei (TH), hypothalamus (HY) and ventral tegmental area (VTA). To rule out confounding systemic vascular changes associated with the pharmacological stimulus and independent of neuronal activity, we also analyzed the signal change in an extracerebral ROI located in the masseter or temporalis muscle.

The "functional" contrast to noise ratio (fCNR) quantifies the sensitivity of the technique as a function of time, since it depends on the USPIO washout rate from the tissue. The fCNR is defined as

$$fCNR(t) = (S_{preCA} - S_0(t))/\sigma_t \quad (5)$$

where S_{preCA} is the pre-contrast baseline signal as defined above, S_0 is the modeled signal recovery using Equation 3 and σ_t is the temporal standard deviation of the signal. Thus, σ_t contains both physical and physiological noise components. To calculate σ_t, we used data acquired during the 5 minute interval that followed contrast agent injection (σ_t of S_{postCA}, Figure 1).

The unpaired Student-Test was used to test the significance ($P < 0.05$) of differences.

Results

During intravenous injection of all three USPIOs, respiratory amplitudes increased and rates increased to about 160 breaths per minute, but both returned to baseline within one minute. In phMRI experiments, we administered cocaine intraperitoneally to avoid sudden hypervolemia and to avoid the body motion that often accompanied intravenous cocaine administration. An IP dose of 30 mg/kg cocaine transiently reduced and then increased the respiratory amplitude for 1 to 3 minutes.

Table 1 lists the contrast agent relaxivities measured at 37°C. In all relaxation time measurements, the linear correlation coefficient of the curve fit was larger than 0.98. Of the three evaluated USPIOs, P904 had the highest transverse relaxivities. With $r_2/r_1 = 60$ at 7T and $r_2/r_1 = 148$ at 11.7T, P904 displayed the most favorable relaxation properties ($r_2 \gg r_1$) for a R_2*-weighted MRI technique.

Figure 2a shows that MION (35 mg/kg) and MoldayION (25 mg/kg) yield similar regional signal changes in the caudate putamen (ROI area 3.2 ± 0.2 mm^2). Doses of 15 mg/kg of P904 decreased signal by about half as much. Increasing the P904 dose to 25 mg/kg yielded a fractional signal decrease of 0.139 ± 0.007, 0.329 ± 0.007, 0.479 ± 0.003 and 0.591 ± 0.003 in the same ROI for TE = 2.5, 6, 9.5 and 13 ms, respectively.

The average fCNR following MION injection was 31.3 ± 6.5, 48.9 ± 9.7, 75.5 ± 6.2, and 112.0 ± 8.8 for TE = 2.5, 6, 9.5 and 13 ms, respectively. Although the signal decrease is significantly greater at TE = 13 ms than at TE = 9.5 ms, the signal decrease induced by the MION injection at TE = 9.5 ms comes closest to the optimal value of $1 - e^{-1}$ (4). We therefore analyzed the ΔCBV in the phMRI experiments using the 3rd echo at TE = 9.5 ms, which displays less macroscopic susceptibility artifact than the 4th echo image at TE = 13 ms. The measured signal decrease not only depends on the USPIO relaxivity and dose, but also on the tissue region examined. The ΔR_2^* map in Figure 2b, calculated according to Eq. 2, also represents the relative local CBV, assuming a linear relationship between CBV and ΔR_2^* (27).

The fCNR varies only slowly during the pharmacological challenge. In the caudate putamen, the average apparent tissue half-life $\tau \cdot \ln 2$ (Figure 3a) was 80 to 90 minutes for 25 mg/kg P904 and 130 to 160 minutes for 35 mg/kg MION. However there was large inter-individual variability. MoldayION (25 mg/kg) caused a sustained susceptibility perturbation in tissue that provided a signal that was practically constant during the duration of the experiment (2 hours post injection). Therefore the tissue washout rate of this USPIO could not be determined accurately in this experiment. Even at TE = 2.5 ms, the tissue half-life was estimated to be at least 7 h. The USPIO half-life is dependent on the injected dose, visible in Figure 3a comparing two P904 doses.

The maps in Figure 3b and c show that the apparent tissue half-life of the USPIO is region specific implying that the signal in each voxel or region needs to be detrended individually. Global detrending of the signal time course using an average apparent washout rate would greatly compromise the quantification of the hemodynamic changes under study. Therefore, prior to quantitative analysis, the signal intensity after contrast agent injection, S(t), was detrended using Eq. 3 to eliminate the effect of contrast agent washout. Equation 3 results in more accurate fits to the signal from individual voxels compared to a constrained exponential model (28) and compared to a two parameter exponential model in which only S_{preCA} is constrained while S_{postCA} is a fitting parameter (Figure 4). Both models result in practically identical S_0 for a signal averaged over larger ROIs or for longer TE (higher fCNR), conditions under which S_{postCA} for the constrained exponential model (28) can be accurately determined.

Neither intraperitoneal nor intravenous injection of saline induced any CBV changes (Figure 5a). A spatially and temporally dependent CBV change was observed in cerebral tissue of mice treated with cocaine. Moreover, there was no measurable effect on extra-cerebral vasculature (Figure 5b). Cocaine induced a CBV decrease (Figure 6) that lasted 40 to 60 minutes with regional differences in amplitude and response time. The largest response amplitudes were observed in ventral and dorsal striatum. To validate the vascular origin of the signal change, we used the carbonic anhydrase inhibitor acetazolamide to dilate cerebral vessels directly. The ΔCBV in response to acetazolamide was slower and more variable between animals but consistently positive (Figure 5b and 6a). As expected, a blood volume increase in extracerebral tissue was also observed in response to acetazolamide (Figure 5b). Figure 6b shows coronal ΔCBV maps from one representative animal in 10 minute intervals before and after the drug challenges. For each map, five time points (5 minutes) were averaged. From these maps, one can see that the striatum, and in particular the ventral

striatum/nucleus accumbens, exhibited the strongest response to cocaine. This response lasted more than 45 minutes. Substantial cocaine-induced CBV changes in the frontal cortex returned to baseline more rapidly. As expected, the CBV increase due to acetazolamide was more uniform across brain regions than that noted for cocaine.

Discussion

Several advantages of the CBV technique have been discussed elsewhere (1, 4, 7, 29). Compared to BOLD imaging, the CBV weighted signal origin is better characterized. Increased fCNR can be achieved even at high magnetic fields (7). ΔCBV assessments after pharmacological challenges provide quantitative parameters that can be compared between individual mice, because they are normalized to the ΔR_2^* drop induced by the USPIO injection prior to the pharmacological challenge. Experimental variations in USPIO dosage or relaxivity or in total mouse blood volume do not impact ΔCBV values, although they do influence the fCNR and thus the sensitivity of the measurement.

In mice, gradient echo acquisitions are less frequently used than T_2-weighted spin echo acquisitions, because susceptibility artifacts generated at tissue air interfaces have a larger impact relative to the small brain size impeding signal analysis in particular brain regions. However, gradient echo acquisitions are potentially more sensitive to the T_2^*-shortening effect of USPIO, hereby increasing the fCNR. To improve the sensitivity of the spin echo technique to vascular changes high contrast agent doses in the order of 1 mmol/kg (50 – 70 mg Fe/kg) were used in some studies (30, 31). Furthermore, it has been shown that spin echo techniques underestimate the cerebrovascular response when using USPIOs (32). In this study, we therefore aimed at establishing a fast gradient echo acquisition protocol and at optimizing the echo time in order to achieve a good fCNR without excessive susceptibility artifacts at the anatomical locations of interest.

All three USPIO have high r_2/r_1 ratios and are suitable contrast agents for CBV weighted phMRI exploiting the transverse relaxation rate changes. Both the signal decrease and the apparent tissue half-life are dose dependent. For doses above 25 mg/kg P904 or MoldayION and 35 mg/kg MION, we achieved a satisfactory fCNR. With apparent tissue half-lives of at least 1.5 hours at these doses, all three USPIO are appropriate for monitoring sustained hemodynamic responses to pharmacological stimuli that benefit from relatively constant fCNR over time.

The given tissue half-lives only approximately reflect the blood half-lives of the USPIO because the signal drop and signal change over time are exponential functions of the USPIO concentration in any voxel. This issue is further complicated by T_1 relaxation effects. However, in an ROI containing a very small blood volume fraction (~ 3%), the USPIO concentration in the ROI is relatively low and the signal drop is approximately proportional to the contrast agent concentration. Under these conditions, the half-life of the tissue signal recovery can be used to estimate the USPIO blood half-life. Although the apparent tissue half-lives of the contrast agents are not significantly different at the chosen echo times, there is a tendency toward increased values at longer echo times, best visible for the lower P904 dose. The echo time dependency represents a complete suppression of the intravascular signal after USPIO injection that masks the gradual decrease in the tissue relaxation rates based on contrast agent washout. Although the acquisition with the shortest echo time would give the closest estimation of the USPIO blood half-life, this measure has a low fCNR. These experiments show the advantage of using a high USPIO dose achieving signal saturation at a particular TE in addition to a prolonged blood half-life. Although our example below employs dynamic imaging with a time resolution of 1 minute, it is possible to achieve true steady state imaging for up to 30 minutes without any detectable signal

change due to contrast agent washout from the blood pool using TE ≥ 9.5 ms with contrast agent doses above 25 mg/kg P904 or MoldayION. This will be important in many applications that require long acquisition times, such as 3D imaging.

Probing brain response to psychotropic drugs is an important and revealing application of neuroimaging (33) in general and phMRI (2, 34), in particular. The cortico-mesolimbic dopaminergic circuit is thought to mediate the rewarding effects of many drugs of abuse, including cocaine. In our example using cocaine challenge in normal mice, we observed the largest negative responses in the nucleus accumbens, followed by caudate putamen and frontal and parietal cortex; all structures with dopaminergic innervations that are important for reward circuit activities (33). The negative ΔCBV response to cocaine challenge is rapid (~15 min) throughout the reward circuit, but relatively long lasting (~45 minutes). To ensure that these measurements inform about neuroactivity we performed a negative and a positive control experiment. To demonstrate that phMRI directly measures changes in blood volume, we examined vascular response to acetezolamide, a potent vasodilator (35). As expected, in this positive control experiment, phMRI indicates that increased cerebral and extra-cerebral blood volume changes are induced by injection of the vasodilator. In a negative control experiment we determined muscle tissue blood volume response to cocaine simultaneously with the cerebral blood volume response to cocaine. Any significant systemic effect of cocaine injection would have resulted in a signal change in muscle tissue, which was not observed. Our findings suggest that the measured CBV change in the current study is independent of systemic effects of the drug. However, the possibility of cocaine interfering directly with the microvascular mechanisms that give rise to the phMRI signal cannot be excluded (23). Various studies have also shown that a drug can have opposite effects depending on the species, the mouse strain, the age, and on various experimental conditions, such as the choice of anesthesia (see references in (23)).

The mechanism for the ΔCBV response to cocaine is complex involving other neurotransmitters and downstream consequences of the effects produced by cocaine. Comparing maps of the ΔCBV response in monoamine transporter and monoamine receptor knock out mice with normal mice will provide significant insight into the mechanisms of action of cocaine and other drugs of abuse.

Conclusion

In this study we have adapted phMRI methodology to meet the requirements of *in vivo* mouse brain imaging. We optimized USPIO choice and dose to yield a procedure with short echo times and evaluated three contrast agents: P904, a new USPIO from Guerbet Research (Aulnay-Sous-Bois, France), monocrystalline iron oxide nanoparticle (MION) (Massachusetts General Hospital, Boston, MA) and MoldayION (BioPAL, MA). All three studied USPIOs are candidates for CBV weighted phMRI-experiments, with r_2/r_1 ratios ≥ 20 and apparent half-lives ≥ 1.5 h at the described doses. An echo time of about 10 ms or longer results in a fCNR > 75 after USPIO injection, with negligible decrease during 1.5 to 2 hours as shown in Figure 5a).

We have applied the phMRI protocol to map the hemodynamic response to cocaine demonstrating the applicability of the CBV weighted phMRI technique to mapping hemodynamic effects of centrally acting drugs in mice. The technique is minimally invasive and provides good functional sensitivity. The negative ΔCBV response to cocaine challenge is rapid (~15 min) throughout the reward circuit. The largest responses to cocaine (−20%ΔCBV) are seen in the nucleus accumbens. Thus these results emphasize the importance of the nucleus accumbens at early as well as later stages of drug exposure. We also note that the mechanisms underlying the CBV changes may not be exclusively specific

to neuroactivation, and necessitate further investigation to separate more direct influences on vasculature from those that are specifically neurovascular.

Acknowledgments

The authors thank Hargun Sohi and Thomas Ng for their technical assistance, Davit Janvelyan for help with the AIR software, and Guerbet Research (Aulnay-Sous-Bois, France) for providing the P904 contrast agent. George Uhl and Scott Hall (National Institute on Drug Abuse, Intramural Research Program) for discussions concerning reward pathway. This project was funded in part by the Beckman Institute, NIDA R01DA18184, and NCRR U24 RR021760 Mouse BIRN.

Abbreviations

MRI	Magnetic Resonance Imaging
phMRI	pharmacological Magnetic Resonance Imaging
CBV	cerebral blood volume
ΔCBV	change in cerebral blood volume
IP	intraperitoneal injection
IV	intravenous injection
USPIO	ultrasmall superparamagnetic iron oxide particles
BOLD	blood oxygen level dependent
SNR	signal to noise ratio
CNR	contrast to noise ratio
fCNR	functional contrast to noise ratio
SEM	standard error of the mean
TE	echo time
T_1	longitudinal relaxation time
T_2	transverse relaxation time
ECG	electrocardiogram
mm	millimeter
mg	milligram
μl	microliter
μs	microsecond
nm	nanometer
ROI	region of interest
MION	monocrystalline iron oxide nanoparticles
FWHM	full width at half maximum
AIR	Automated Image Registration
CA	contrast agent
CTX	somatosensory cortex
ACB	nucleus accumbens

CP	caudate putamen
HPF	hippocampal formation
TH	thalamic nuclei
HY	hypothalamus
VTA	ventral tegmental area

References

1. Chen YC, Mandeville JB, Nguyen TV, Talele A, Cavagna F, Jenkins BG. Improved mapping of pharmacologically induced neuronal activation using the IRON technique with superparamagnetic blood pool agents. J Magn Reson Imaging. 2001; 14(5):517–24. [PubMed: 11747003]
2. Martin C, Sibson NR. Pharmacological MRI in animal models: A useful tool for 5-HT research? Neuropharmacology. 2008; 55(6):1038–1047. [PubMed: 18789342]
3. Jenkins BG, Sanchez-Pernaute R, Brownell AL, Chen YCI, Isacson O. Mapping Dopamine Function in Primates Using Pharmacologic Magnetic Resonance Imaging. J Neurosci. 2004; 24(43): 9553–9560. [PubMed: 15509742]
4. Mandeville JB, Marota JJ, Kosofsky BE, Keltner JR, Weissleder R, Rosen BR, Weisskoff RM. Dynamic functional imaging of relative cerebral blood volume during rat forepaw stimulation. Magn Reson Med. 1998; 39(4):615–24. [PubMed: 9543424]
5. Schwarz AJ, Gozzi A, Reese T, Heidbreder CA, Bifone A. Pharmacological modulation of functional connectivity: the correlation structure underlying the phMRI response to d-amphetamine modified by selective dopamine D-3 receptor antagonist SB277011A. Magnetic Resonance Imaging. 2007; 25(6):811–820. [PubMed: 17442525]
6. Weissleder R, Elizondo G, Wittenberg J, Lee AS, Josephson L, Brady TJ. Ultrasmall superparamagnetic iron oxide: an intravenous contrast agent for assessing lymph nodes with MR imaging. Radiology. 1990; 175(2):494–8. [PubMed: 2326475]
7. Mandeville J, Jenkins B, Chen Y, Choi J, Kim Y, Belen D, Liu C, Kosofsky B, Marota J. Exogenous contrast agent improves sensitivity of gradient-echo functional magnetic resonance imaging at 9.4 T. Magn Reson Med. 2004; 52:1272–1281. [PubMed: 15562489]
8. Luo F, Seifert TR, Edalji R, Loebbert RW, Hradil VP, Harlan J, Schmidt M, Nimmrich V, Cox BF, Fox GB. Non-invasive characterization of beta-amyloid(1–40) vasoactivity by functional magnetic resonance imaging in mice. Neuroscience. 2008; 155(1):263–9. [PubMed: 18534764]
9. Mueggler T, Baumann D, Rausch M, Staufenbiel M, Rudin M. Age-dependent impairment of somatosensory response in the amyloid precursor protein 23 transgenic mouse model of Alzheimer's disease. Journal of Neuroscience. 2003; 23(23):8231–8236. [PubMed: 12967984]
10. Wu EX, Tang HY, Asai T, Du Yan S. Regional cerebral blood volume reduction in transgenic mutant APP (V717F, K670N/M671L) mice. Neuroscience Letters. 2004; 365(3):223–227. [PubMed: 15246553]
11. Gainetdinov RR, Caron MG. Monoamine transporters: From genes to behavior. Annual Review of Pharmacology and Toxicology. 2003; 43:261–284.
12. Girault JA, Greengard P. The neurobiology of dopamine signaling. Archives of Neurology. 2004; 61(5):641–644. [PubMed: 15148138]
13. Shen T, Weissleder R, Papisov M, Bogdanov A Jr, Brady TJ. Monocrystalline iron oxide nanocompounds (MION): physicochemical properties. Magn Reson Med. 1993; 29(5):599–604. [PubMed: 8505895]
14. Matsumoto S, Hyodo F, Subramanian S, Devasahayam N, Munasinghe J, Hyodo E, Gadisetti C, Cook JA, Mitchell JB, Krishna MC. Low-field paramagnetic resonance imaging of tumor oxygenation and glycolytic activity in mice. The Journal of Clinical Investigation. 2008; 118(5): 1965–1973. [PubMed: 18431513]
15. Sigovan M, Boussel L, Sulaiman A, Sappey-Marinier D, Alsaid H, Desbleds-Mansard C, Ibarrola D, Gamondes D, Corot C, Lancelot E, Raynaud JS, Vives V, Lacledere C, Violas X, Douek PC,

Canet-Soulas E. Rapid-clearance iron nanoparticles for inflammation imaging of atherosclerotic plaque: initial experience in animal model. Radiology. 2009; 252(2):401–9. [PubMed: 19703881]

16. Jamshidi HR, Rezayat M, Zarrindast MR. Effect of apmin on tolerance to cocaine-induced locomotor activity in mice. Acta Medica Iranica. 2004; 42(2):78–82.
17. Rocha BA, Fumagalli F, Gainetdinov RR, Jones SR, Ator R, Giros B, Miller GW, Caron MG. Cocaine self-administration in dopamine-transporter knockout mice. Nat Neurosci. 1998; 1(2): 132–7. [PubMed: 10195128]
18. Mateo Y, Budygin EA, John CE, Jones SR. Role of serotonin in cocaine effects in mice with reduced dopamine transporter function. Proc Natl Acad Sci U S A. 2004; 101(1):372–7. [PubMed: 14691264]
19. Berry I, Benderbous S, Ranjeva J, Gracia-Meavilla D, Manelfe C, Le Bihan D. Contribution of Sinerem used as blood-pool contrast agent: detection of cerebral blood volume changes during apnea in the rabbit. Magn Reson Med. 1996; 36:415–419. [PubMed: 8875412]
20. Woods RP, Grafton ST, Holmes CJ, Cherry SR, Mazziotta JC. Automated image registration: I. General methods and intrasubject, intramodality validation. J Comput Assist Tomogr. 1998; 22(1): 139–52. [PubMed: 9448779]
21. Abramoff MD, Magelhaes PJ, Ram SJ. Image Processing with ImageJ. Biophotonics International. 2004; 11(7):36–42.
22. Paxinos, G.; Franklin, K. The Mouse Brain in Stereotaxic Coordinates. 2. San Diego: Academic Press; 2001. p. 296
23. Perles-Barbacaru TA, Procissi D, Demyanenko AV, Hall FS, Uhl GR, Jacobs RE. Quantitative pharmacologic MRI: Mapping the cerebral blood volume response to cocaine in dopamine transporter knockout mice. Neuroimage. 2011; 55(2):622–628. [PubMed: 21185387]
24. Perles-Barbacaru, AT.; Procissi, D.; Demyanenko, AV.; Jacobs, RE. Nonlinear model for preprocessing of cerebral blood volume weighted functional MRI data and for evaluating pharmacokinetic properties of USPIO. Proc. Intl. Soc. Mag. Reson. Med. 18th Annual Scientific Meeting; Stockholm (Sweden). 2010.
25. Nicolaysen LC, Pan HT, Justice JB Jr. Extracellular cocaine and dopamine concentrations are linearly related in rat striatum. Brain Res. 1988; 456(2):317–23. [PubMed: 3208083]
26. Thompson D, Martini L, Whistler JL. Altered Ratio of D1 and D2 Dopamine Receptors in Mouse Striatum Is Associated with Behavioral Sensitization to Cocaine. PLoS One. 2010; 5(6):9.
27. Wu EX, Tang H, Asai T, Yan SD. Regional cerebral blood volume reduction in transgenic mutant APP (V717F, K670N/M671L) mice. Neurosci Lett. 2004; 365(3):223–7. [PubMed: 15246553]
28. Schwarz AJ, Reese T, Gozzi A, Bifone A. Functional MRI using intravascular contrast agents: detrending of the relative cerebrovascular (rCBV) time course. Magn Reson Imaging. 2003; 21(10):1191–200. [PubMed: 14725926]
29. Mandeville JB, Marota JJ. Vascular filters of functional MRI: spatial localization using BOLD and CBV contrast. Magn Reson Med. 1999; 42(3):591–8. [PubMed: 10467305]
30. Mueggler T, Sturchler-Pierrat C, Baumann D, Rausch M, Staufenbiel M, Rudin M. Compromised hemodynamic response in amyloid precursor protein transgenic mice. J Neurosci. 2002; 22(16): 7218–24. [PubMed: 12177216]
31. Princz-Kranz FL, Mueggler T, Knobloch M, Nitsch RM, Rudin M. Vascular response to acetazolamide decreases as a function of age in the arcA beta mouse model of cerebral amyloidosis. Neurobiol Dis. 2010; 40(1):284–92. [PubMed: 20600914]
32. Mandeville JB, Leite FP, Marota JJ. Spin-echo MRI underestimates functional changes in microvascular cerebral blood plasma volume using exogenous contrast agent. Magn Reson Med. 2007; 58(4):769–76. [PubMed: 17899605]
33. Koob GF, Volkow ND. Neurocircuitry of Addiction. Neuropsychopharmacology. 2010; 35(1): 217–238. [PubMed: 19710631]
34. Schwarz AJ, Zocchi A, Reese T, Gozzi A, Garzotti M, Varnier G, Curcuruto O, Sartori I, Girlanda E, Biscaro B, Crestan V, Bertani S, Heidbreder C, Bifone A. Concurrent pharmacological MRI and in situ microdialysis of cocaine reveal a complex relationship between the central hemodynamic response and local dopamine concentration. Neuroimage. 2004; 23(1):296–304. [PubMed: 15325377]

35. Supuran CT. Carbonic anhydrases: novel therapeutic applications for inhibitors and activators. Nat Rev Drug Discov. 2008; 7(2):168–181. [PubMed: 18167490]

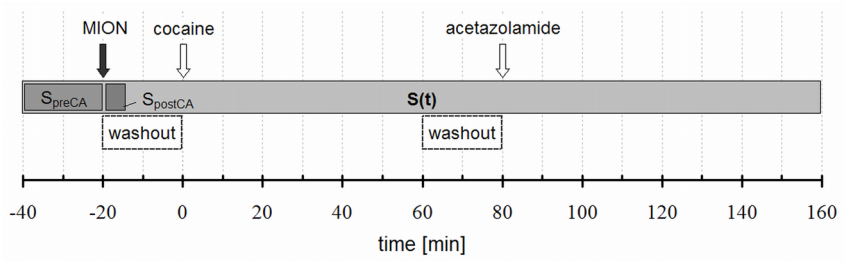

Figure 1.

Experimental phMRI protocol: gradient echo images were acquired continuously with a time resolution of 1 minute. USPIO was delivered IV to sensitize the MR signal to CBV followed by cocaine (30 mg/kg IP) and the vasodilator acetazolamide (160 mg/kg IP). $S_{preCA.}$ is the constant baseline signal before contrast agent injection; S_{postCA} is the average of five consecutive signals acquired immediately after contrast agent injection; and S(t) is the time dependent CBV-weighted signal after contrast agent injection. The time intervals marked as washout were used to detrend the signal and to derive the contrast agent washout rate.

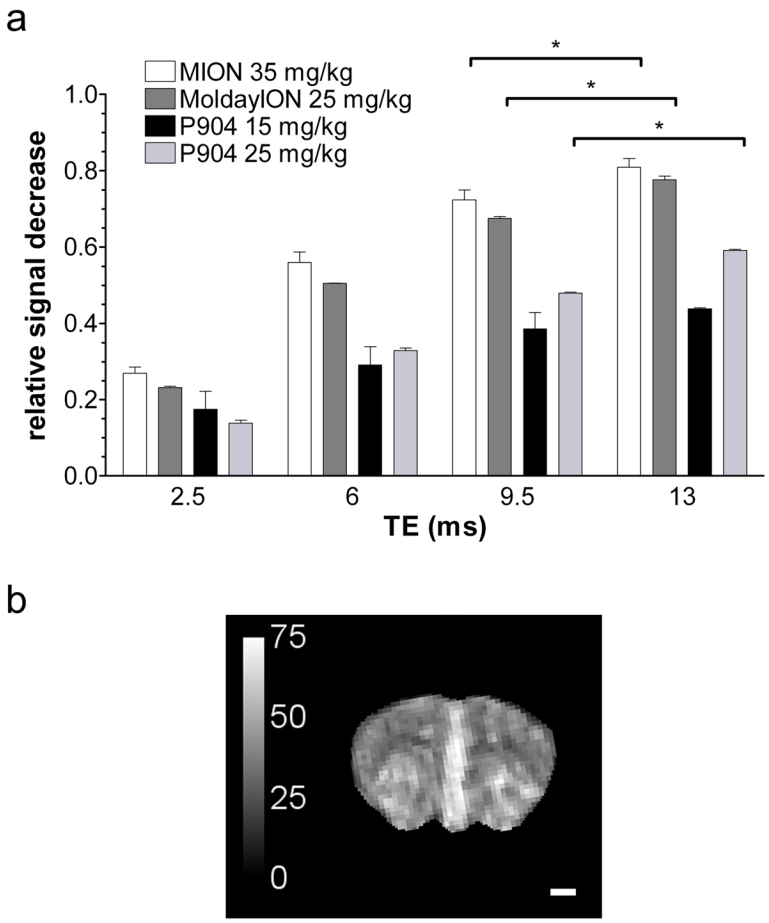

Figure 2.

a) Average signal decrease ± standard error of the mean (SEM) in cerebral tissue (caudate putamen, 3.2 ± 0.2 mm^2) after IV USPIO. b) Representative coronal ΔR_2*-map (bregma + 1 mm, 0.18 × 0.18 × 0.75 mm^3 voxel size) resulting from 35 mg/kg MION injection that is proportional to the local CBV. Scale bar is 1 mm. Intensity scale is in s^{-1}.

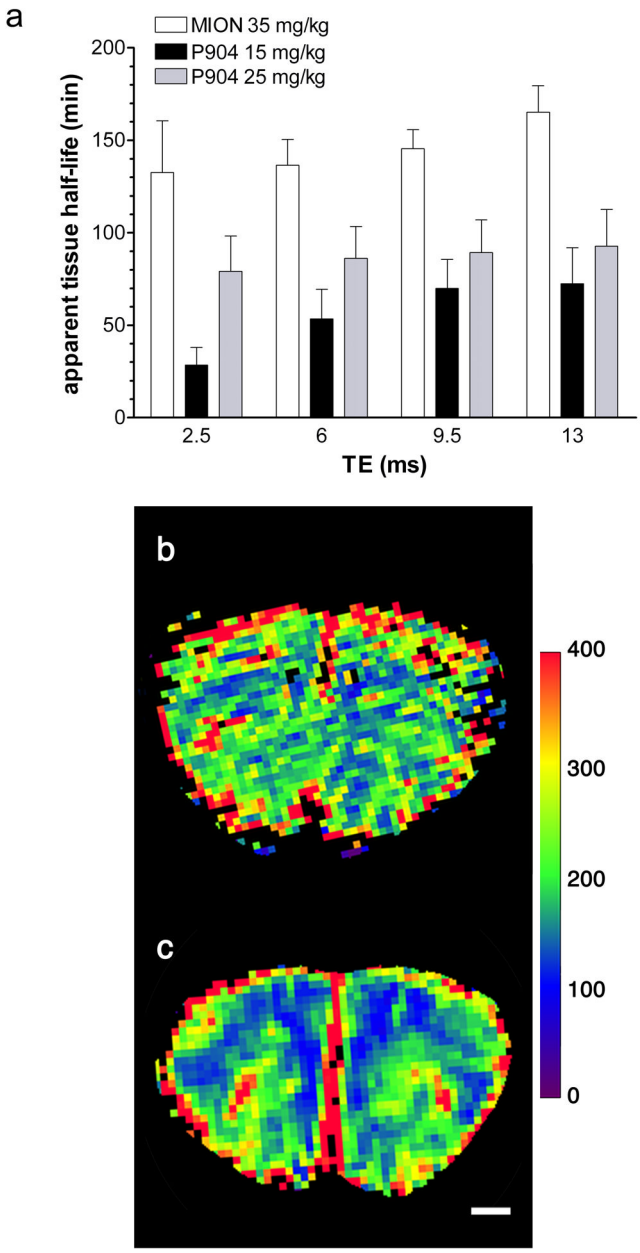

Figure 3.

a) Average apparent USPIO half-life (τ·ln2) ± SEM in minutes in the caudate putamen. Apparent tissue half-life of MoldayION is not shown, but was estimated to be > 7 hr (cf. main text). b and c) Representative maps of the apparent tissue half-life for 35 mg/kg MION (b) and for 25 mg/kg P904 (c). Black pixels represent failed fit. Intensity scale is in minutes. Scale bar is 1 mm.

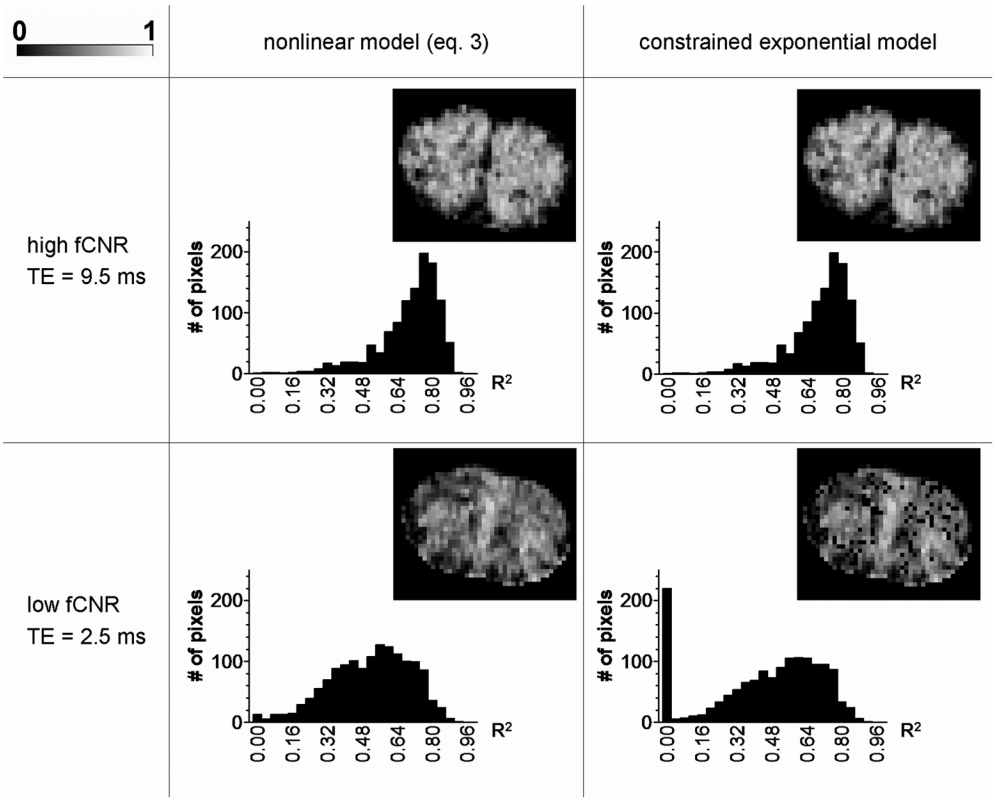

Figure 4.

Comparison of the nonlinear two parameter fit (Eq. 3) and an exponential constrained two parameter fit (28) for voxelwise detrending of high and low fCNR data. The four maps and the histograms show a basic parameter of the goodness of fit (R^2) for 1446 voxels located in brain tissue. Black voxels represent failed fit. The intensity scale is $0 \leq R^2 \leq 1$.

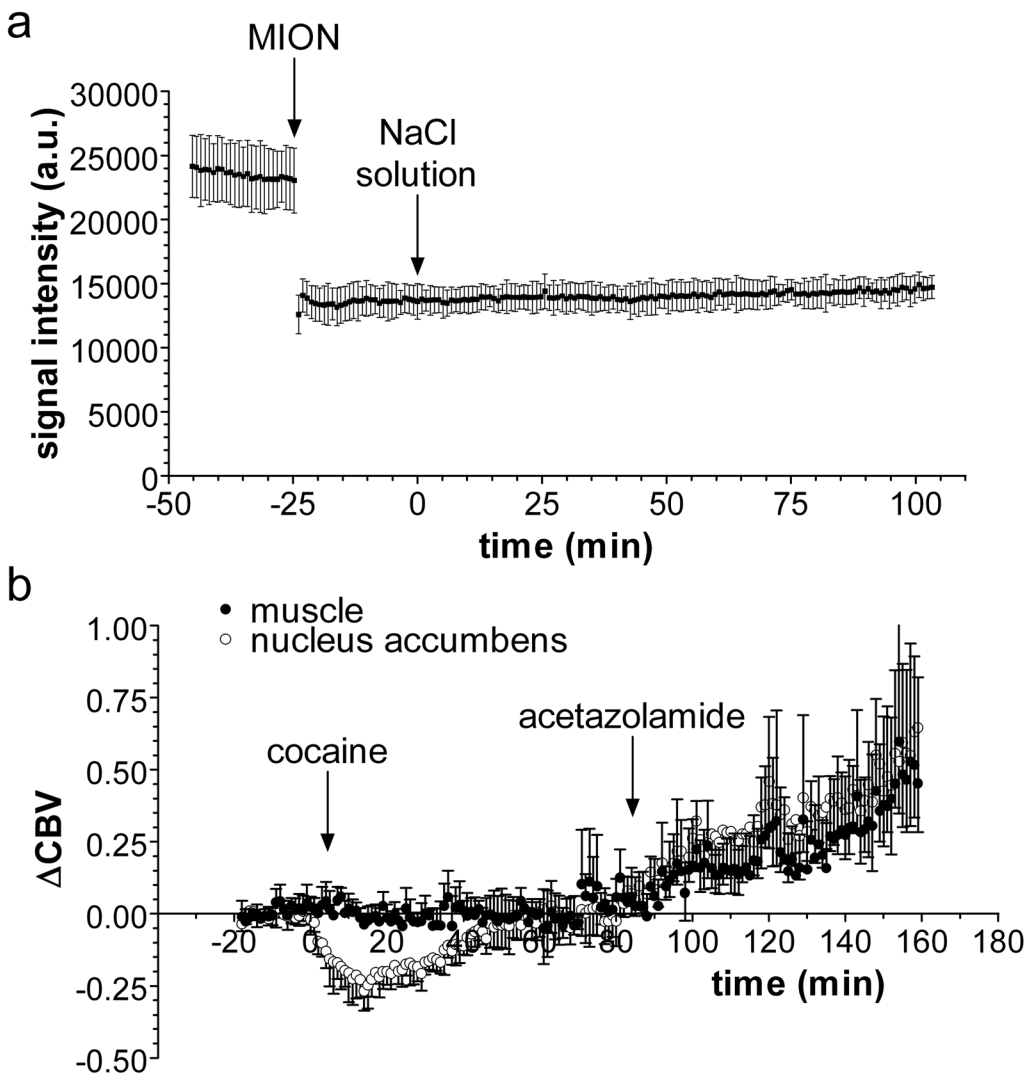

Figure 5.

a) Typical signal time course from a ROI in the ACB (area 2.5 mm^3) in a single mouse. Error bars show the standard deviation of the signal within the ROI. IV injection of normal saline solution (10 μl/g) induces no hemodynamic effect in brain tissue. b) Effect of IP cocaine (30 mg/kg) and acetazolamide (160 mg/kg) on the time course of the ΔCBV in cerebral (ACB) and in extra-cerebral tissue (muscle). Injection of cocaine leads to a CBV decrease in cerebral tissue without hemodynamic effect in extracerebral tissue, while vasodilation is observed in cerebral and extra-cerebral tissues after acetazolamide injection. Error bars show the standard deviation (N = 5).

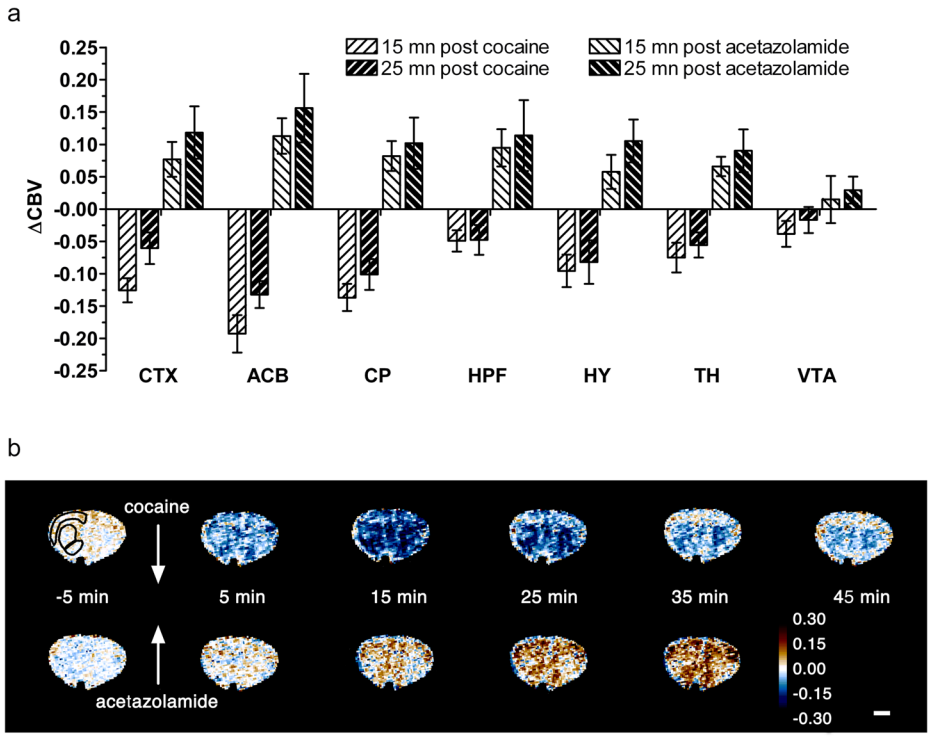

Figure 6.

a) ROI analysis shows that injection of 30 mg/kg cocaine IP causes local decreases in the CBV in mice, while injection of 160 mg/kg acetazolamide IP causes global vasodilation. Typically, the ΔCBV response peaks at 15 min after cocaine injection, while the vasodilatory effect of acetazolamide is slower and more variable. The error bars represent the standard error of the mean (N = 5). For each time point the signal was averaged over 5 minutes. b) Representative coronal maps (bregma + 1 mm) of the CBV change (ΔCBV) averaged over 5 minutes at different time-points after IP cocaine injection. The strongest and fastest CBV changes occur in ventral striatum/ACB after both drugs. Differential CBV changes can be observed in dorsal striatum and frontal cortex. The three ROIs outlined on the leftmost map are CTX, CP and ACB (dorsal to ventral). Intensity scale is fractional ΔCBV. Scale bar is 2 mm.

Table 1

in vitro longitudinal and transverse relaxivities in $s^{-1}mM^{-1}$ in rat plasma at 37°C

		7T	11.7T
MION	r_1	2.38 ± 0.03	1.12 ± 0.01
	r_2	48. 7 ± 1.2	60.6 ± 0.6
P904	r_1	1.42 ± 0.02	0.64 ± 0.01
	r_2	85 ± 1.3	94.7 ± 0.8
MoldayION	r_1	1.99 ± 0.01	1.01 ± 0.02
	r_2	67.5 ± 0.4	81. ± 1.5